Photogrammetric techniques for monitoring tunnel deformation

**M. Scaioni · L. Barazzetti · A. Giussani · M. Previtali ·
F. Roncoroni · M. I. Alba**

Introduction

Nowadays, the maintenance of the safety conditions during construction and serviceability of infrastructures is a topic attracting more and more attention. This is due to the remark-able relevance that different typologies of communication corridors play in modern society, with direct impact on the social and economic development. Among different aspects, structural health monitoring is a crucial task (Brownjohn 2007) requiring the combination of different measurement techniques to provide sufficient information to analyse defor-mations and predict possible collapses. Thus, several sensors are used for structural monitoring. These feature different properties in terms of accuracy, cost, time needed for their set up and so on (Ou and Li 2010; Sun et al. 2010; Aygün and Gungor 2011; Cigada et al. 2011; Merlino and Abramo 2011; Mukhopadhyay and Ihara 2011; Afzal et al. 2012; Liu

and Kleiner 2012; Jang et al. 2012; Jindal and Mingyan 2012; Yi and Li 2012; Guarnieri et al. 2013; Schotte et al. 2013; Yi et al. 2013).

Deformation monitoring with conventional engineering geodesy techniques plays an important role. They allow the high-precision observation of displacements regarding some control points which are permanently fixed to the structure. Both manual and automatic approaches are employed. The selection depends on many factors, like period of monitoring, risk for people potentially involved in a collapse, shape and dimensions of the object, required measurement accuracy, budget, number and spatial distribution of the investigated points. For these reasons there are many applications where manual measurements are steadily used, for example when infrastructures are subject to temporary works that actively or passively have an effect on the stability.

In this paper the monitoring of tunnels is focused, whose structural safety is an important field of research in Civil Engineering. Generally speaking, it comprehends the analysis of several factors and the creation of ad-hoc solutions which should guarantee rapid measurements with sufficient accuracy.

Two complementary photogrammetric techniques for the measurement of tunnel deformations are illustrated. They are based on the use of images to reconstruct 3D geometry (Luhmann et al. 2013). Imagery and laser scans have been already exploited for surveillance and inspection purposes in tunnels (see Guo et al. 2011; Sandrone 2013). The solutions developed here would like to deal with some crucial aspects during tunnel construction, serviceability and maintenance: the measurement of relative deformations in transversal tunnel cross-sections (Section Measurement of deformations in tunnel cross-sections), and the measurement of relative and absolute vertical displacements along the longitudinal profile (Section Photogrammetric levelling). Normally, both problems are faced on the basis of engineering geodesy techniques. Total stations or tape extensometers are used for the measurement of cross-sections, while optical (or digital) levels are employed within geometric levelling schemes for observing vertical displacements (Schofield and Breach 2007). The photogrammetric methods presented in the following are aimed at overcoming some drawbacks of traditional techniques, especially in the case of underground lines, when time becomes an issue of primary importance and limits the number of measurements that can be accomplished. In many cases, the survey is carried out at night when traffic can be halted in easier way.

Close-range photogrammetric methods have been successfully used in several civil engineering applications involving the determination of the geometric shape of a body and its changes (Fraser and Riedel 2000; Hattori et al. 2002; Whiteman et al. 2002; Fraser et al. 2003; Barazzetti and Scaioni 2010; Fedele et al. 2014). The achievable precision depends upon the size of the investigated element (Maas and

Hampel 2006). For experiments in a controlled environment a relative precision in the order of 1:100,000 of the largest object dimension can be expected, but during analysis in repeatable system configuration (e.g., a multi-epoch test with fixed camera stations) a precision of 1:250,000 was achieved (Maas and Niederöst 1997; Albert et al. 2002). In Fraser et al. (2005) the hyper redundancy network concept was used for the study of surface deformations of a radio telescope, with a precision from 1:580,000 to 1:670,000.

Measurement of deformations in tunnel cross-sections

Measurement of relative deformation in tunnel cross-sections is normally carried out by using special tape extensometers which must be connected to particular stable hooks (Kovari and Amstad 1993). This method allows measuring the reciprocal distance between all hook combinations with a high precision (±0.01 mm). Another system is based on the use of a total station placed on stable supports along the wall of the tunnel. The position of several topographic reflectors mounted along the cross-section is estimated with a precision superior to ±1 mm. Both methods (total station- and tape-based) provide target displacements with an accuracy which is more than sufficient to fulfil the requirements of structural engineers. However, the survey of a single cross-section may take several minutes (approximately 15' depending on the number of targets), because of the time needed to set up the instruments and for observation reading. This means that only few parts of the tunnel can be analysed during time when traffic is interrupted.

Several studies have been accomplished in recent years to improve operational aspects of tunnel deformation monitoring. The most of them are based on the adoption of terrestrial laser scanning sensors, coupled with model fitting methods to interpolate points and reduce the effect of noise (Argüelles-Fraga et al. 2013; Pejić 2013; Tuo et al. 2013). Indeed, the major drawback of such sensors is related to the precision of single point measurement. Many solutions have been developed to reduce the uncertainty by exploiting the very high point density. On the other hand, published results reports about accuracy worse than ±5 mm, and the required instrumentation is still costly.

Methodology

The basic idea of the photogrammetric approach is based on the use of targets placed on the gallery vault. Images depicting each investigated cross-section will contain all the useful information to determine target positions into a local datum up to an unknown scale ambiguity. This can be defined by measuring the distance between two targets using an invar wire. This method allows one to increase the productivity of

the survey, because the time necessary to acquire the images is less than 2 min and processing can be carried out in office at a later stage. Moreover, it is possible to deploy a large number of control points to obtain a better description of the arch relative deformations in the cross-section plane.

To determine a good compromise in terms of image number and precision, several tests with different network geometries were carried out. A simple solution based on a single strip made up of four images (see Fig. 1) provided satisfactory results. A photographic tripod was used to obtain clear images. A consumer-grade single-lens reflex (SLR) camera was utilised for this application. The adopted camera needed to be calibrated to remove the effects of lens distortion, operation that could be accomplished in the office before or after the survey in the tunnel. Calibration is a simple and standard task that can be operated by the user himself using a set of coded targets (Fraser 2013). After capturing a small set of images (10–15) from different point-of-views, a computer code can be exploited for the automatic measurement of targets' image coordinates, and then to work out the bundle adjustment providing the estimation of the camera calibration parameters. Several low-cost or free software packages are available to this aim.

Data processing consists of three main stages. First of all, targets are independently measured on the images with the *Least Squares Template Matching* (LSTM) algorithm (Grün 1985) in order to obtain subpixel accuracy (up to 1/20 pixel size). Then 3D coordinates of targets are estimated into a local datum within a *free-net* bundle adjustment (Luhmann et al. 2013). Finally, the scale ambiguity is removed and the relative distances between targets computed. During the initial measurement campaign, the distance between two targets close to the floor is measured by using a total station. In the following, the wire readings are used to check if this distance has changed and then to modify the scale accordingly.

Figure 1 shows a 3D view of a typical data acquisition scheme, including the computed control points (targets) and four camera stations. As can be seen, there are some additional removable targets on the floor, which were used to increase the redundancy of the system and to improve the point distribution in the images. After data acquisition these targets can be removed.

Experiments

Test site

A real tunnel was used for different experiments. It was located in Parè di Valmadrera between the towns of Lecco and Bellagio (Lombardia region, Italy). The tunnel was normally closed to regular car traffic and used as a deposit (see Fig. 1).

Figure 2 shows a typical cross-section of this tunnel, which is roughly 12 m wide. Fifteen 'double-face' targets were applied to the vault, but only 9 were used during experiments. A target is made up of a circular black mark with a white background (Figs. 3 and 4). It is mounted on a metal support which is fixed to the tunnel wall with screws. On the opposite side of each control point, a total station target-tape reflector is applied for validation measurements.

In addition, two opposite targets (no. 4 and 12 in Fig. 2) were fixed on supports for connecting the invar wire to measure the distance change between these points (see 4). This is useful for a multi-epoch control: photogrammetric projects have a scale ambiguity that must be removed with an external constraint. The wire used (made of invar steel), coupled with a mechanical gauge, is a cheap and fast solution for determining the variation of distance between these points, given an initial measurement operated by a total station. Moreover, this method has a high accuracy for measuring relative changes (±0.01 mm), more than sufficient if compared to the expected precision of the photogrammetric method (±0.5 mm). During the measurement with the gauge it is also useful to read the temperature inside the tunnel, in order to correct systematic errors due to thermal variations.

The light of the illumination system of the tunnel was used during tests reported in this paper. However, some other experiments proved that the use of additional light sources did not modify the results.

More information on operational and technical details about these experiments can be found in Alba et al. (2010).

Photogrammetric equipment

Two SLR amateur digital cameras were employed in the experiments: a Nikon D80 with a 20 mm Sigma lens and a Nikon D700 with a 35 mm Nikkor lens. Properties of both sensors are reported in Table 1. Special photogrammetric cameras were not taken into account because of their higher cost, although they would probably allow a significant improvement in terms of sensor stability (quite important for a multi-epoch analysis). Cameras were calibrated in the tunnel after the completion of each survey. Here iWitness® (Photometrix, Australia) software package with its complementary calibration targets was used (www.photometrix.com.au).

Benchmarking data

To validate the photogrammetric results, during each measurement campaign all targets were acquired by a total station Leica TCA 2003 (Leica Geosystems). This method is widely used in a lot of real cases and can be assumed as a proven technique, useful to validate the photogrammetric measurements. To achieve accuracy better than ±1 mm in the determination of the target coordinates, a method based on the intersection from two stations was adopted (Schofield and
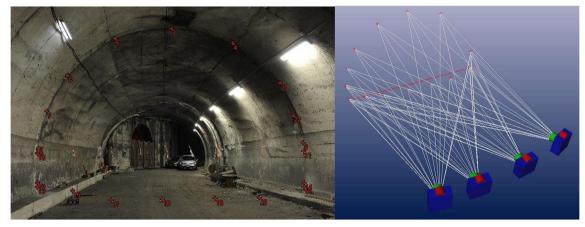
Fig. 1 On the left, an example of application of the photogrammetric method for measuring relative deformations in tunnel cross-sections is shown. On the right, a 3D view showing camera poses and 3D target positions (*red points*) along with the projecting rays

Breach 2007). The instrument was placed on a couple of stable shelves on the opposite sides of the wall of the tunnel. For each station a plate was rigidly fixed to the wall of the gallery. Thus, each shelf can be mounted on the plate at different epochs while the correct positioning is guaranteed by the fixed plate. The photogrammetric method provides relative displacements between the targets on the cross-section. The total station measurements adopted for validation was also used to derive relative measurements. For this reason, possible displacements of the walls where plates were fixed did not affect the measurement of relative deformations, because the local datum was established at each epoch by using EDM measurements between stations. In addition, the invar wire was adopted to check possible deformations between both walls of the tunnel in correspondence of any observation campaign. A theoretical precision of about ±0.2 mm along both in-plane directions were achieved for the target of the cross-section. This resulted in a precision of relative distances between targets of about ±0.3 mm.

Single-epoch deformation measurement

The first test was carried out to determine the accuracy of the method during a single measurement session. Here, some displacements could be given to a target placed on the floor by using a bi-directional micrometric sledge. Their magnitude was measured with two analogue comparators (accuracy ±0.01 mm). The sledge allows the simulation of planar movements by using some micrometric screws.

This test is based on the simulation of a displacement in the cross-section plane. This kind of deformation is also the most likely to occur in real applications. A strip of four images was acquired as shown in Fig. 1. Then, a displacement was given with the micrometric screw and a new image sequence was taken. This experiment was repeated several times at the same epoch, in order to avoid systematic errors due to camera stability. Globally, the experiment took less than 15 min.

Table 2 shows the results related to a typical situation: four displacement steps were given with the sledge (+1, +1, −1 and −1 mm) and their magnitude was estimated with the photogrammetric approach based on the use of a Nikon D700/35 mm Nikkor lens camera. As can be seen, the discrepancy between measurements was less than ±0.3 mm and confirmed the accuracy of this method. Moreover, the closure error (+0.22 mm) was quite good and made this result satisfactory in terms of accuracy.

Multi-epoch deformation measurement

In real applications for tunnel safety monitoring, measurements are normally gathered at different epochs. Here, the major concern related to the applicability of the photogrammetric method is the stability of the adopted camera along time, while control points can be rigidly fixed to the concrete structure and are supposed to be fully stable. In fact, SLR digital cameras must be calibrated at every epoch to remove systematic errors. To assess this point, four datasets were
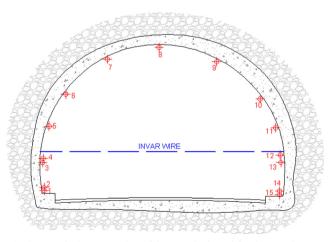

Fig. 2 A typical cross-section of the tunnel adopted for the experiments. Small crosses indicate the positions of targets on the vault

Fig. 3 The 'double-face' control point adopted for both photogrammetric and theodolite measurements

taken in different months in order to obtain a temporal window of approximately 30 days between consecutive epochs. Both digital cameras reported in Table 1 were employed. During the periods between the measurement campaigns in the tunnel, cameras were used for other works in order to worsen their stability and simulate real operational conditions. Distances d_{ij} between all target pair combinations were derived at each epoch by using photogrammetry. Thus, measurements at epoch t were compared with those at next epoch $t+1$:

$$\left(\Delta d_{ij}\right)_{ph}^{t,t+1} = \left(d_{ij}\right)_{ph}^{t+1} - \left(d_{ij}\right)_{ph}^{t} \qquad (1)$$

to obtain 'photogrammetric' variations. Contemporarily, a total station was utilised to acquire benchmarking data within a similar approach.

The comparison was carried out by analysing the differences of variations achieved with both techniques (sub-index 'ph' stands for 'photogrammetry' and 'ts' for 'total station'):

$$\left(\delta_{ij}\right)^{t,t+1} = \left(\Delta d_{ij}\right)_{ph}^{t,t+1} - \left(\Delta d_{ij}\right)_{ts}^{t,t+1} \qquad (2)$$

In the case of Nikon D80 camera, targets were pictured in windows larger than 18×18 pixels in the images. Four epochs

were used to check the quality of the photogrammetric measurements. As can be seen from the results in Table 3, there is a positive systematic error confirmed by the fact that means are larger than standard deviations of the departures between observations from both methods. The magnitude of this error is larger than the expected accuracy (±0.5 mm).

The same experiment was repeated with the superior quality camera Nikon D700. This sensor has a metal body that is naturally more robust and supposed to be stable overtime. In this case, the size of each target in the images was about 23× 23 pixels.

The analysis of the images taken at three epochs provided the results shown in Table 4. As can be seen, the systematic effect was reduced and the standard deviation of the difference of variations gives a value less than 0.5 mm.

To complete this analysis, theoretical precisions from the estimated covariance matrix of the bundle adjustment of the photogrammetric block are considered. These resulted in $\sigma_Y = \sigma_Z = 0.1$ mm for in-plane directions and $\sigma_X = 0.2$ mm in off-plane direction. To compare these values with the ones in Table 4, precisions on point coordinates were propagated to work out the precision of relative distances. Roughly, these resulted about $\sigma_d = 0.14$ mm, value that is still better than the empirical one. On the other hand, the uncertainty of benchmarking values is very close to the nominal accuracy

Fig. 4 The invar wire and the gauge used to remove the scale ambiguity from the photogrammetric project

Table 1 Technical properties of cameras adopted in experiments

camera	Type of camera	Sensor	Lens	Sensor size	Pixel size
Nikon D80	SLR	CCD	Sigma 20 mm	2,896×1,944 pix 23.6×15.8 mm	8.1 μm
				3,872×2.592 pix 23.6×15.8 mm	6.1 μm
Nikon D700	SLR	CMOS	Nikkor 35 mm	3,872×2.592 pix 13.2×8.8 mm	9.3 μm
				4,256×2,832 pix 36×24 mm	8.4 μm

of total station data, and then these outcomes can be considered as satisfactory. Moreover, experimental results demonstrated an accuracy of about ±0.5 mm for a tunnel wider than 12 m (1:24,000) that seems to suffice for real surveys.

Photogrammetric levelling

Geometric (or *spirit*) *levelling* is still undoubtedly the most used method for the measurement of vertical deformations in man-made structures like bridges, historical buildings, dams, and the like. This is motivated by the limited cost of the equipment and its sub-millimetre precision (Schofield and Breach 2007).

In the case of applications for tunnel monitoring, geometric levelling provides the relative vertical displacements of a series of benchmarks deployed along the longitudinal profile of the infrastructure to form a line. The absolute heights with respect to a reference point outside the tunnel can be found by summing up all relative differences. This allows the determination of height changes for data taken at different epochs.

One of the main drawbacks of precise levelling is the low measurement speed, with a productivity limited to a small number of points per hour (about 10 point/h, depending upon the operational conditions and the surveyor's expertise). In some applications aimed at determining the safety state of a structure, time becomes a paramount factor and limits the number of points that can be checked. In the case of road or railway tunnel monitoring, for example, measurements need to be rapidly carried out during the night, when traffic is stopped.

In latest years, the use of digital levels helped speed up the measurement process and made it less dependent on the surveyor's ability. But analogue levels with parallel plate glass micrometres are still used in several high-precision applications because of their high performances. This solution may provide readings with a precision of ±0.1 mm for 1 cm graduations on the rods that can be then estimated up to ±0.01 mm.

In the following of this section a solution aimed at speeding up levelling campaigns is introduced and validated against the traditional technique. The key concept is to replace the standard equipment by introducing an innovative image-based solution, which is notably faster and even more economical. The proposed method has been termed as 'photogrammetric levelling'.

Methodology

The estimation of the height difference between two points can be carried out with a calibrated camera and a couple of special photogrammetric rods. The camera must be calibrated beforehand as already discussed in the previous application in Section Measurement of deformations in tunnel cross-sections. The employed rods had a length of 150 cm and the typical graduation was replaced by 3 circular targets. Targets can be automatically recognized and registered in each image with subpixel precision. The camera is placed in front of the rods to acquire data from the middle position. The attitude of the camera does not require particular care. On the other hand, rods are placed on benchmarks and are quasi vertical thanks to a heavy mass that is connected at the bottom end. This is the fundamental difference between the standard optical levelling approach (where the optical or digital level gives a horizontal line of sight) and the 'photogrammetric levelling' (where two rods provide the vertical direction and the attitude of the camera can be variable). The camera should be placed at

Table 2 The relative displacements detected with the photogrammetric method and benchmarking values

Epochs	Relative displacement steps	Measured displacements (Nikon D700/35 mm lens)	Differences
0 – 1	+1 mm	0.78 mm	0.22 mm
1 – 2	+1 mm	1.11 mm	−0.11 mm
2 – 3	-1 mm	−0.82 mm	−0.18 mm
3 – 4	−1 mm	−0.85 mm	−0.15 mm
Closure error	0 mm	+0.22 mm	
Statistics on differences w.r.t. benchmarking data		Mean	−0.06 mm
		Std.dev.	0.19 mm

Table 3 Statistical comparison between relative distances obtained from photogrammetry (Nikon D80 camera) and total station measurements

	Epoch 0–1	Epoch 1–2	Epoch 2–3
Mean (mm)	0.23	0.66	0.88
Std.dev (mm)	0.57	0.60	0.53
RMS (mm)	0.62	0.89	1.03

approximately the same distance from each rod in order to remove some systematic errors. As shown in Fig. 5, the camera height should be about the same of the middle target on the rods.

A couple of parallel rods form a parallelogram in space (see Fig. 6). When rods are depicted in the image, the shape of this parallelogram is changed mainly due to camera lens distortions and perspective deformations. The former effect can be compensated for by applying camera calibration parameters. The latter can be taken into account with the estimation of a 2D homography, i.e., a projective transformation with 8°-of-freedom. Indeed, rods in object space define a plane and they can be mapped into the image by using such 2D homography. This can be represented by a 3×3 non-singular *homography matrix* (Hartley and Zisserman 2004):

$$\mathrm{x} = \begin{bmatrix} x \\ y \\ 1 \end{bmatrix} = \begin{bmatrix} h_1 & h_2 & h_3 \\ h_4 & h_5 & h_6 \\ h_7 & h_8 & h_9 \end{bmatrix} \begin{bmatrix} X \\ Y \\ 1 \end{bmatrix} = \mathbf{H}\mathbf{X} \tag{3}$$

where points in image $\mathrm{x} = [x\, y\, 1]^{\mathbf{T}}$ and object space $\mathrm{X} = [X\, Y\, 1]^{\mathbf{T}}$ are expressed in homogenous coordinates.

A common method for the estimation of matrix **H** is based on a set of point-to-point x↔X correspondences (at least four), which however cannot be employed to take over the traditional levelling approach, as the coordinates in object space are unknown.

The 'photogrammetric levelling' is based on the method for parallelogram rectification proposed in Barazzetti (2011), who demonstrated that the knowledge of the vanishing line in the image coupled with the constraints available from camera calibration may suffice to recover metric properties up to an unknown 2D similarity transformation.

Most digital cameras equipped with CCD or CMOS sensors follow the central perspective (or pinhole) model, which

Table 4 Statistical comparison between relative distances obtained from photogrammetry (Nikon D700 camera) and total station measurements

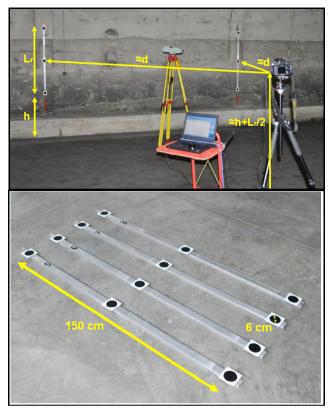|	Epoch 0–1	Epoch 1–2
Mean (mm)	0.00	−0.06
Std.dev (mm)	0.32	0.32
Max (mm)	0.78	0.65

Fig. 5 An example of the basic operational scheme of 'photogrammetric levelling' with two rods hung on benchmarks and a digital camera (at the *top*), along with some examples of the special targeted rods (at the *bottom*)

expresses a mathematical relationship between image (x) and object (X) points through a 3×4 *projection matrix* **P** (Hartley and Zisserman 2004):

$$\mathrm{x} = \begin{bmatrix} x \\ y \\ 1 \end{bmatrix} = \mathbf{P} \begin{bmatrix} X \\ Y \\ Z \\ 1 \end{bmatrix} = \mathbf{P}\mathbf{X} \tag{4}$$
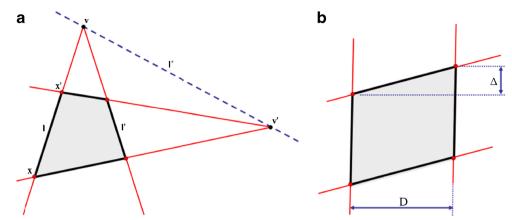
The projection matrix **P** can be decomposed into the matrix product:

$$\mathbf{P} = \mathbf{K}[\mathbf{R}\ \ \mathbf{t}] \tag{5}$$

where:

$$\mathbf{K} = \begin{bmatrix} c & 0 & x_0 \\ 0 & c & y_0 \\ 0 & 0 & 1 \end{bmatrix} \tag{6}$$

is called *calibration matrix* and encapsulates the interior orientation parameters of the camera (principal distance c and principal point coordinates x_0, y_0) that are available from camera calibration; **R** is the *rotation matrix* and the vector t

Fig. 6 Geometric quantities used to rectify the original image (**a**) and the estimated values (**b**)

contains the coordinates of the perspective center (Luhmann et al. 2013).

Collins and Beveridge (1993) demonstrated that the orientation of the object plane with respect to the camera can be estimated if both *vanishing line* l* and calibration matrix **K** are known. The image coordinates x and x′ of rod targets (see Figs. 5 and 6) allow the estimation of a line as:

$$l = x \times x' \tag{7}$$

A vanishing point v can be estimated by using the intersection of a couple of parallel lines l and l′:

$$v = l \times l' \tag{8}$$

In the current application, the two vertical lines defined by targets on each rod are used to compute the vanishing point v, and the three parallel lines defined by the corresponding targets at the bottom, middle and top position of each rod are used to define v′. The vanishing line of the plane is computed by using two vanishing points v and v′:

$$l^* = v \times v' \tag{9}$$

The normal unary vector of the image plane (u_n) with respect to the object can be derived as follows:

$$u_n = \frac{n}{\|n\|} = \frac{\mathbf{K}^T 1^*}{\|\mathbf{K}^T 1^*\|} \tag{10}$$

This vector is adopted to define the camera rotation matrix $\mathbf{R} = [u_r \, u_s \, u_n]^{\mathbf{T}}$, which is made up of three orthonormal vectors. Being u_n already known from Eq. (10), others can be computed by exploiting the normality and orthogonality constraints, as demonstrated in Barazzetti (2011).

The homography matrix **H** in Eq. (3) is then:

$$\mathbf{H} = \mathbf{KRK}^{-1} \tag{11}$$

From inversion of Eq. (3), coordinates of targets in object space X′ can be worked out up to an unknown similarity transformation:

$$X' = \begin{bmatrix} X' \\ Y' \\ 1 \end{bmatrix} = \begin{bmatrix} \lambda\cos\alpha & \lambda\sin\alpha & t_X \\ -\lambda\sin\alpha & \lambda\cos\alpha & t_Y \\ 0 & 0 & 1 \end{bmatrix} \begin{bmatrix} X \\ Y \\ 1 \end{bmatrix} = \mathbf{H}_S X \tag{12}$$

where absolute shifts t_x and t_y are not required for the estimation of relative height differences (arbitrary values can be employed), the global scale factor λ can be obtained from the real distance between targets on the rods, and α depends on the transformed image coordinates.

Figure 7 shows both original and rectified images. As can be noticed, image distortion has been removed by resampling the original images using the camera calibration model. This solution has been adopted here only to better show the operational procedure, while in real applications images are not resampled to maintain the original image quality and to avoid low-pass filtering. To deal with distortions on the images, numerical values of coordinates are corrected before estimating the homography.

The final step is the estimation of the height difference:

$$\Delta = Y'_3 - Y'_1 = Y'_4 - Y'_2 \tag{13}$$

This value is assumed as the difference between the heights of benchmarks where rods are hung up.

Optionally, also the horizontal distance between rods can be computed:

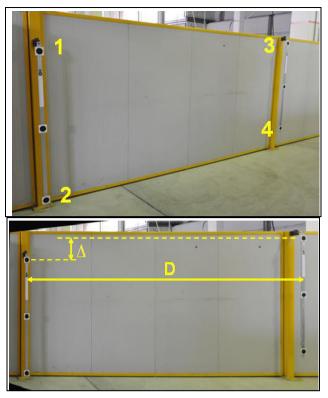$$D = X'_3 - X'_1 = X'_4 - X'_2 \tag{14}$$

Fig. 7 A distortion-free image of the rods' setup (at the *top*) and its corresponding rectified image (at the *bottom*)

This last value cannot be measured with a standard levelling procedure.

Experiments

Application with synthetic data

A set of 20 synthetic images generated with 3D Studio Max® was used to check the correctness of the implemented algorithms (measurement of targets' centres and rectifying homography). The distortion-free images were created assuming a 6 megapixel camera equipped with a 20 mm lens that were virtually acquired from different stations. The imaged scene is quite simple, as only two vertical rods are visible. During the 'virtual' acquisition of the images, rods were moved along both horizontal and vertical directions to simulate different displacements. The magnitude of displacements is therefore completely known and can be used to validate the results of 'photogrammetric levelling'. In a few words, the simulated horizontal (D_i^s) and vertical distances (Δ_i^s) were compared to those estimated using the image-based procedure (D_i^{pl}, Δ_i^{pl}).

The length of the simulated rod, i.e., the distance between targets, is 150 cm. The horizontal distance ranged from 4 to 6 m and images were taken not only from the middle, but also from decentered positions in order to obtain narrow angles of view. Departures between simulated and estimated values

($d_i=D_i^s-D_i^{pl}$, $\delta_i=\Delta_i^s-\Delta_i^{pl}$) provided $\mu(d_i)\pm\sigma(d_i)=-0.08\pm$ 0.08 mm for horizontal and $\mu(\delta_i)\pm\sigma(\delta_i)=0.04\pm0.07$ mm for vertical displacements, respectively. They confirmed a relative accuracy of 1:40,000, although a systematic error is evident from the mean values. In any case, the geometry used during these tests was more complicated than in real applications, where images are supposed to be taken from the middle position.

A note about the use of 3D Studio Max® for simulating images has to be made. Indeed, the principle of image formation in this software is not well known, although it is expected to follow the central perspective model. For instance, which method is implemented for assigning the radiometric value to each pixel is not clear (nearest neighbor, bilinear or higher order interpolation, etc.). These aspects should be deeper investigated for future applications of such kind of image simulation. On the other hand, here the aim is to compute relative differences, so that possible systematic effects may cancel out.

Laboratory experiments

A second group of tests were performed in a controlled environment using the SLR cameras described in Table 1. During a real monitoring campaign, if images are acquired at different epochs, it is normal to setup the camera approximately at the same position. The first test aimed at determining the height difference (Δ_i^{pl}) between the same benchmarks (rods were fixed) from slightly different standpoints, in order to simulate a multi-temporal data acquisition. The observed elevation difference should be constant. In all, 16 differences were measured by using a camera Nikon D80 equipped with a 20 mm lens. Results are shown in Figs. 8 and 9. The standard deviation of measured values resulted in 0.1 mm that is quite similar to the precision of a good quality optical level.

In the second test several images were taken with a calibrated Nikon D700 equipped with a 35 mm lens and two metal rods hung on benchmarks. A ruler was also applied to each rod in order to measure the height difference with a high-precision optical level Zeiss Ni1 (nominal standard deviation 0.2 mm). As can be seen in Fig. 10c, one rod may change its vertical position to simulate displacements. A set of 20 height differences were applied and corresponding measurements
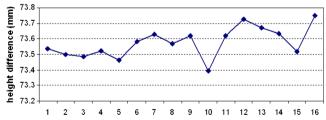

Fig. 8 Values of the height differences measured by placing the camera Nikon D80 on slightly different positions

Fig. 9 From left to right: the lab test setup to compare 'photogrammetric' and optical levelling (**a**); the rod with a ruler to allow readings with the optical level (**b**); and the weight to stabilize each rod (**c**)

carried out by both techniques: optical levelling (Δ_i^{ol}) and 'photogrammetric levelling' (Δ_i^{pl}). The statistic on the differences $d_i = \Delta_i^{ol} - \Delta_i^{pl}$ resulted as $\mu(d_i) \pm \sigma(d_i) = 0.05 \pm 0.09$ mm.

Tunnel experiments

In the last test a real levelling campaign in a tunnel was organized. Both kinds of measurements with 'photogrammetric' and optical levelling were accomplished and results compared. A series of benchmarks were installed along one of the lateral walls (Fig. 10). The photogrammetric rods have a ruler to be also measured with an optical level Zeiss Ni1. A benchmark was equipped with an adjustable screw and an analogue gauge (precision ±0.01 mm) to give some vertical displacements.

Data were collected by using Nikon D700 camera equipped with 35 mm lens. A closed path with 4 benchmarks (in forth and back direction) was followed in order to check the loop-closure error. The 'photogrammetric levelling' provided satisfactory results, as the final closure error was less than 0.2 mm. However, a direct comparison between the simulated displacements based on optical levelling and gauge measurements provided discrepancy superior to 0.4 mm. The cause of this unexpected effect is still not clear and might depend on several factors. Probably, the method is sensitive to the distance

Fig. 10 The experiment in a real tunnel with a sequence of rods hung on benchmarks. On the right side a detail focusing on the adjustable screw to simulate displacements is shown

between the rods, and a rod of 150 cm is not sufficient to cope with distances larger than 5 m. This is an evident limit but its investigation needs more exhaustive analysis. On the other hand, measurements have been operated at the same time by using optical and 'photogrammetric levelling' and temperature cannot be assumed as the reason of such departures. In general, the effect of temperature should be considered, as discussed in subsection Photogrammetric levelling.

Another problem was found when the rod is not stable, especially when it swings like a pendulum due to wind. This is not a serious problem for measurement carried out with a level, which gives a horizontal line of sight. However, the 'photogrammetric levelling' is more sensitive to this effect as rods give the vertical direction. The installation of a heavy weight (5 kg) allows one to strongly reduce this drawback, although level bubbles should be installed on the rods to check their alignment along the plumb line.

Further information on the experiments can be found in Barazzetti et al. (2011).

Discussion

In this session a discussion on both photogrammetric methods for tunnel deformation monitoring is afforded on the basis if the experimental results. The aim is to highlight advantages and limitations of the proposed techniques that first are separately discussed. In the end, some common aspects are analysed together.

Measurements of cross-sections

Several single- and multi-epoch tests were carried out to analyse the performances of this method under different conditions. The single-epoch analysis demonstrated the precision achievable with 4 images taken by moving the camera from the left to the right side of the tunnel. With this configuration an accuracy better than ±0.3 mm was reached for a tunnel wider than 12 m. The multi-epoch analysis showed some issues related to the stability of the camera and its calibration. However, a good SLR digital camera was sufficient to reach an accuracy of approximately ±0.5 mm, which is suitable for most real applications.

The method provides relative displacements between targets, which must be carefully fixed to the structure because possible movements may lead to detect false displacements. On the other hand, in the experience of the authors a proper installation of targets is not a problematic issue (see Scaioni et al. 2010). Each section is analysed independently from others. This means that relative changes between two sections cannot be detected, but other solutions are needed to this purpose. For example, coupling the measuring of cross-sections and levelling (also by using the 'photogrammetric'

approach) may give a more complete overview on the general deformation of the tunnel structure. The longitudinal spacing between observed cross-sections is another aspect to be carefully planned as trade-off between cost/time of monitoring and expected results.

The use of the invar wire is required to check possible displacements between two targets that are used to define the scale of the photogrammetric reconstruction. The distance is measured during the first observation campaign by using a total station. In the following epochs only changes need to be evaluated by using the invar wire. Such solution is not the optimal one, because the installation of the invar wire and the system for its tensioning is time consuming. In the future, alternative solutions have to be developed, for example by using a removable calibrated invar bar instead of the wire. This method would be quite simple under an operational point-of-view, but at the same time would guarantee a high-precision. Another option is related to the implementation of this technique along with a mobile mapping vehicle (Tao and Li 2007). Here one or more cameras could move along a calibrated track installed on the roof of the vehicle. This solution does not require to measure any distance on the object, because the exterior orientation of the camera stations could be independently computed beforehand.

Photogrammetric levelling

The precision in experiments carried out under controlled conditions was satisfactory (±0.1÷0.2 mm), although in a real tunnel application some unexpected results were found (discrepancies with respect to benchmarking values up to 0.4 mm). This still limits the use of the photogrammetric levelling approach in real cases and makes new analyses necessary to better understand the behavior of the method and possible sources of errors.

As the discussion on the camera quality is reported in subsection Common aspects, here the focus is on the rod design. During experiments temperature was quite stable and also regular steel rods did not result in significant thermal deformation. Generally, however, the adopted rods (150 mm length) may elongate up to 0.2 mm under a $\Delta T=10$ C. The adoption of invar rods would strongly reduce the same effect to less than 0.02 mm under the same conditions.

The 'photogrammetric levelling' has the potential to speed up surveying operations in the field and to be installed on mobile mapping vehicle for high-productivity surveys. It can be applied along with the adjustment model of standard levelling networks where optical/digital levels are used. Relative height changes between two benchmarks can be measured, but it may also provide absolute changes if several simple observations are connected in a network and referred to one or more stable points.

On the other hand, more investigations on systematic errors and validation of the technical equipment have to be seriously carried out before the application of this methodology in real-world tunnels (or other kinds of structures). The validation procedure proposed in this paper can be followed as guideline to setup the assessment of other implemented solutions.

Common aspects

The methods proposed for measuring deformations in tunnels have both an experimental character and cannot be intended yet as ready solutions to be used in the monitoring practice. Tunnels and infrastructures where they are supposed to be applied are capital objects and need reliable, fully proved and certified techniques and instruments to monitor their static stability. On the other hand, they have the potential to be used as alternatives to standard techniques in some applications where lower precision is needed in relative measurements and where a high-degree of automation and productivity are required (for example in mobile mapping vehicles). The use of cameras makes also possible their implementation in permanent monitoring systems, where the application of geodetic instruments (e.g., robotic total stations) is still expensive. Anyway, a careful design of the equipment and a complete and rigorous validation are called for.

The selection of the equipment plays an important role, especially about the camera to apply. It is not straightforward to give some criteria to select a specific camera rather than another. Results of experiments in paragraph 2.2.5 showed how large differences could be found by using two different SLR cameras. A bias up to 0.88 mm was found in the distances between targets obtained with a Nikon D80 and a higher quality Nikon D700 camera. This problem seemed to be related to the stability of the CCD or CMOS sensor inside the camera. A careful selection and some pre-validation tests have to be accomplished before starting the real application.

Calibration is also an essential task to remove systematic errors due to lens distortion. This operation, which is quite simple at the current state-of-the-art of close-range photogrammetry, has to be repeated in occasion of every measurement campaign. Also in this case, a set of calibration parameters may have different time validity in relation with the stability of the sensor in the camera. In the experiments carried out in this paper the camera was setup on a topographic tripod, whose function was to keep the camera stable during shooting and to avoid blurring effects in the images. On the other hand, both methods do not require capturing the image from exactly the same stand-points, so the stability of the tripod overtime is not a relevant issue.

Conclusion

In this paper a couple of photogrammetric methods for deformation measurements in tunnels have been introduced to overcome some drawbacks of the state-of-art techniques. These new solutions have been designed to reduce the time needed for data acquisition in the field. Indeed, time is an important limiting constrain when operating in situations requiring halting the regular car or train traffic. Moreover, the photogrammetric equipment is surely cheaper than topographic instruments that are usually adopted in these kinds of engineering surveys.

The first method addressed is focused on the measurement of cross-section relative deformations. It is based on the use of a calibrated single-lens reflex (SLR) digital camera, a set of targets to be permanently installed on the tunnel vault, and an invar wire (or a calibrated bar) to fix the scale ambiguity. If a stable SLR digital camera is applied, an accuracy of ±0.5 mm roughly can be reached, which is suitable for most real applications.

In the second part, an image-based approach ('photogrammetric levelling') for monitoring vertical displacements in tunnels has been presented. This method has been specifically designed for tunnel monitoring applications, where rods can be hung up to benchmarks deployed along the tunnel walls. Although a satisfying precision was obtained in experiments under controlled conditions, the application for multi-epoch monitoring in a real tunnel showed a high sensibility to some factors like the length of the rod and the camera type. Further investigations are needed to overcome existing problem and obtain the same reliability of optical/digital levelling.

The applicability of the proposed image-based techniques to other kinds of structures (e.g., historical buildings, bridges, dams,…) would need specific investigations because of the different geometry and environmental conditions.

References

Afzal MHB, Kabir S, Sidek O (2012) An in-depth review: structural health monitoring using fiber optic sensor. IETE Tech Rev 29(2): 105–113

Alba M, Barazzetti L, Giussani A, Roncoroni F, Scaioni M (2010) Development and testing of a method for tunnel monitoring via vision metrology. Int Arch Photogramm Remote Sens Spat Inf Sci 38(5):17–22

Albert J, Maas HG, Schade A, Schwarz W (2002) Pilot studies on photogrammetric bridge deformation measurement. Proc. of 2nd IAG Int. Symp. on Geodesy for Geotechnical and Structural Engineering, Berlin, Germany, pp. 133–140

Argüelles-Fraga R, Ordóñez C, García-Cortés S, Roca-Pardiñas J (2013) Measurement planning for circular cross-section tunnels using terrestrial laser scanning. Autom Constr 31:1–9

Aygün B, Gungor VC (2011) Wireless sensor networks for structural health monitoring: recent advances and future research. Sens Rev 31(3):261–276

Barazzetti L (2011) Planar metric rectification via parallelograms. In Proc. of Int. Conf. Videometrics, Range Imaging, and Applications XI, 23−26 May 2011, Munich, Germany (Proc. of SPIE, Vol. 8085, No. 80850R), 12 pages (e-doc)

Barazzetti L, Scaioni M (2010) Development and implementation of image-based algorithms for measurement of deformations in material testing. Sensors 10(8):7469–7495

Barazzetti L, Roncoroni F, Alba IM, Giussani A, Previtali M, Scaioni M (2011) Photogrammetric Levelling. In Proc. of Joint Int. Symp. on Deformation Monitoring, 2–4 Nov, Hong-Kong, S.A.R. China, 6 pages (e-doc)

Brownjohn JMW (2007) Structural health monitoring of civil infrastructure. Phil Trans R Soc A 365:589–622

Cigada A, Comolli L, Giussani A, Roncoroni F, Zenucchi F (2011) *Thermal characterization of FBG strain gauges for the monitoring of the cupola of Duomo di Milano*. Proc. SPIE 7753, 21st International Conference on Optical Fiber Sensors, 775380 (May 17, 2011)

Collins RT, Beveridge JR (1993) Matching perspective views of coplanar structures using projective unwarping and similarity matching. Proc. of Conf. on Computer Vision and Pattern Recognition (CVPR'93), 15–17 June, New York, NY-USA, pp. 240–245

Fedele R, Scaioni M, Barazzetti L, Rosati G, Biolzi L, Condoleo P (2014) Delamination tests on CFRP-reinforced masonry pillars: optical monitoring and mechanical modelling. Cem Concr Compos 45: 243–254

Fraser CS (2013) Automatic camera calibration in close range photogrammetry. Photogramm Eng Remote Sens 79:381–388

Fraser CS, Riedel B (2000) Monitoring the thermal deformation of steel beams via vision metrology. ISPRS J Photogramm Remote Sens 55(4):268–276

Fraser CS, Brizzi DV, Hira AR (2003) Vision-Based Multi-Epoch Deformation Monitoring of the Atrium of Federation Square. In Proc. of 11th FIG Symp. on Deformation Measurements, Santorini, Greece, pp. 599–604

Fraser CS, Woods AR, Brizzi DV (2005) Hyper redundancy for accuracy enhancement in automated close range photogrammetry. Photogramm Rec 20(111):205–217

Grün A (1985) Adaptative least squares correlations: a powerful matching techniques. S Afr J Photogramm Remote Sens Cartogr 14(3):175–187

Guarnieri A, Milan N, Vettore S (2013) Monitoring of complex structures for structural control using terrestrial laser scanning (TLS) and photogrammetry. Int J Archit Herit 7(1):54–67

Guo Y, Shi H, Yu Z (2011) Research on tunnel complete profile measurement based on digital photogrammetry technology. In Proc. of 2011 I.E. Int. Conf. on Service Operations, Logistics and Informatics (SOLI 2011), pp. 521−526

Hartley RI, Zisserman A (2004) Multiple view geometry in computer vision, 2nd edn. Cambridge University Press, Cambridge, 672 pages

Hattori S, Akimoto K, Fraser C, Imoto H (2002) Automated procedures with coded targets in industrial vision metrology. Photogramm Eng Remote Sens 68(5):441–446

Jang S, Dahal S, Contreras GK, Fitch J, Karamavros J, Bansal R (2012) Hybrid structural health monitoring for in-service highway bridges using wireless multiscale sensors. In SPIE Smart Structures and Materials+ Nondestructive Evaluation and Health Monitoring (pp. 83451Y-83451Y)

Jindal A, Mingyan L (2012) Networked computing in wireless sensor networks for structural health monitoring. Netw IEEE/ACM Trans 20(4):1203–1216

Kovari K, Amstad C (1993) Decision making in tunnelling based on field measurements. Compr Rock Eng Bergamon 4:571–606

Liu Z, Kleiner Y (2012) State-of-the-art review of technologies for pipe structural monitoring. IEEE Sensors J 12(6):1987–1992

Luhmann T, Robson S, Kyle S, Böhm J (2013) Close Range Photogrammetry: 3D Imaging Techniques. Walter De Gruyter Inc., 702 pages

Maas HG, Hampel U (2006) Photogrammetric techniques in civil engineering material testing and structure monitoring. Photogramm Eng Remote Sens 72(1):39–45

Maas HG, Niederöst M (1997) The accuracy potential of large format still video cameras. In Proc. of Videometrics V, 27 July, San Diego, CA-USA, SPIE Proceedings Series No. 3174

Merlino P, Abramo A (2011) Deformation detection in structural health monitoring. Lect Notes Electr Eng 96:41–62

Mukhopadhyay SC, Ihara I (2011) Sensors and technologies for structural health monitoring: a review. Lect Notes Electr Eng 96:1–14

Ou J, Li H (2010) Structural health monitoring in mainland China: review and future trends. Struct Health Monit 9(3):219–231

Pejić M (2013) Design and optimisation of laser scanning for tunnels geometry inspection. Tunn Undergr Space Technol 37:199–206

Sandrone F (2013) Tunnel conditions assessment based on image analysis: a new inspection procedure for railways tunnels. In Proc. of World Tunnel Congress 2013, Geneva, Switzerland, pp. 459−465

Scaioni M, Alba IM, Giussani A, Roncoroni F (2010) Monitoring of a SFRC retaining structure during placement. Eur J Environ Civil Eng 14(4):467–493

Schofield W, Breach M (2007) Engineering Surveying, 6th Edition. Butterworth-Heinemann, Oxford

Schotte K, De Backer H, Nuttens T, De Wulf A, Van Bogaert P (2013) Strain gauge measurements of the precast concrete lining of a shield-driven tunnel. Insight Non-Destruct Test Cond Monit 55(2):88–95

Sun M, Staszewski WJ, Swamy RN (2010) Smart sensing technologies for structural health monitoring of civil engineering strcutures. Advances in Civil Engineering, art. no. 724962

Tao CV, Li J (2007) Advances in Mobile Mapping Technology: ISPRS Series, Vol. 4. Francis & Taylor, 192 pages

Tuo L, Kang Z, Xie Y, Wang B (2013) Continuously vertical section abstraction for deformation monitoring of subway tunnel based on terrestrial point clouds. Geomatics Inf Sci Wuhan Univ 38(2):171−175+185

Whiteman T, Lichti D, Chandler I (2002) Measurement of deflections in concrete beams by close range photogrammetry. Int Arch Photogramm Remote Sens Spat Inf Sci Vol. 34(4), on CD-ROM

Yi TH, Li HN (2012) Methodology development in sensor placement for health monitoring of civil infrastructures. Int J Distrib Sensors, art. no. 612726

Yi TH, Li HN, Gu M (2013) Recent research and applications of GPS-based monitoring technology for high-rise structures. Struct Control Health Monit 20(5):649–670